Gas-Phase Kinetics and Mechanism of the Reactions of Protonated Hydrazine with Carbonyl Compounds. Gas-Phase Hydrazone Formation: Kinetics and Mechanism

Thomas G. Custer,[†] Shuji Kato,[†] Veronica M. Bierbaum,[†] Carleton J. Howard,[‡,§] and Glenn C. Morrison*,[‡,||,⊥]

Contribution from the Department of Chemistry and Biochemistry, University of Colorado, 215 UCB, Boulder, Colorado 80309-0215, National Oceanic and Atmospheric Administration (NOAA), Aeronomy Laboratory R/AL2 325 Broadway, Boulder, Colorado 80305, Cooperative Institute for Research in Environmental Sciences, University of Colorado, Boulder, Campus Box 216, Boulder, Colorado 80309

Received March 10, 2003; E-mail: gcm@umr.edu

Abstract: The gas-phase reactions of protonated hydrazine (hydrazinium) with organic compounds were studied in a selected ion flow tube−chemical ionization mass spectrometer (SIFT-CIMS) at 0.5 Torr pressure and ∼300 K and with hybrid density functional calculations. Carbonyl and other polar organic compounds react to form adducts, e.g., $N_2H_5^+(CH_3CH_2CHO)$. In the presence of neutral hydrazine, aldehyde adducts react further to form protonated hydrazones, e.g., $CH_3CH_2CH=HNNH_2^+$ from propanal. Using deuterated hydrazine (N_2D_4) and butanal, we demonstrate that the gas-phase ion chemistry of hydrazinium and carbonyls operates by the same mechanisms postulated for the reactions in solution. Calculations provide insight into specific steps and transition states in the reaction mechanism and aid in understanding the likely reaction process upon chemical or translational activation. For most carbonyls, rate coefficients for adduct formation approach the predicted maximum collisional rate coefficients, $k \sim 10^{-9}$ cm^3 molecule^{-1} s^{-1}. Formaldehyde is an exception ($k \sim 2 \times 10^{-11}$ cm^3 molecule^{-1} s^{-1}) due to the shorter lifetime of its collision complex. Following adduct formation, the process of hydrazone formation may be rate limiting at thermal energies. The combination of fast reaction rates and unique chemistry shows that protonated hydrazine can serve as a useful chemical-ionization reagent for quantifying atmospheric carbonyl compounds via CIMS. Mechanistic studies provide information that will aid in optimizing reaction conditions for this application.

Introduction

Hydrazine and its derivatives are invaluable analytical reagents and their chemistry in solution has been studied extensively.[1] It has long been recognized that these species react uniquely with carbonyl compounds. Emil Fischer[2] was the first to report the use of phenyl hydrazine for the detection of carbonyl compounds in solution. Later, Purgotti[3] used 2,4-dinitrophenylhydrazine (DNPH) to quantify aldehydes. DNPH is still widely used for sensitive measurements of carbonyl compounds in aqueous solutions and in extracted air samples.[4] The carbonyl derivatization reaction (an addition process) is similar for all substituted hydrazine compounds. Scheme 1

Scheme 1. Acid-Catalyzed Hydrazone Formation in Condensed Phase
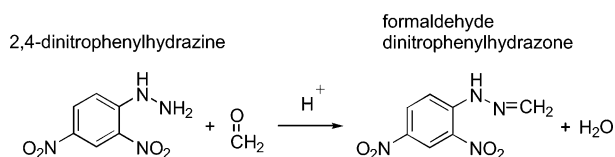
shows the acid-catalyzed DNPH derivatization of formaldehyde to produce formaldehyde hydrazone with the elimination of water. The resulting hydrazones are readily detected by the strong absorption of visible light by the nitrophenyl chromophore.

Despite its long history in solution, only a few studies have investigated the gas-phase ion chemistry of hydrazine or the hydrazinium ion. Generally such studies are related to combustion chemistry and the use of hydrazine as a fuel. The unimolecular decomposition of $N_2H_5^+$ was studied by Oiestad and Uggerud[5] using both theory and experiment. Feng et al.[6]

[†] Department of Chemistry and Biochemistry, University of Colorado.
[‡] National Oceanic and Atmospheric Administration.
[§] Retired, current e-mail address: cjhome@comcast.net.
[||] Cooperative Institute for Research in Environmental Sciences, University of Colorado.
[⊥] Current address: Department of Civil Engineering, 221 Butler-Carleton Hall, University of Missouri−Rolla, Rolla, MO 65409-0030.-

(1) Sollenberger, P. Y.; Martin, R. B. In *The Chemistry of the Amino Group*; Patai, S., Ed.; John Wiley & Sons: New York, 1968; Vol. 1, pp 349−407.
(2) Fischer, E. *Chem. Ber.* **1884**, *17*, 572−584.
(3) Purgotti, A. *Gazz. Chem. Ital.* **1894**, *24*, 554−584.
(4) Zhou, X.; Mopper, K. *Environ. Sci. Technol.* **1990**, *24*, 1482−1485.

(5) Oiestad, E. L.; Uggerud, E. *Int. J. Mass Spectrom. Ion Processes* **1997**, *165/166*, 39−47.
(6) Feng, W. Y.; Aviyente, V.; Varnali, T.; Lifshitz, C. *J. Phys. Chem.* **1995**, *99*, 1776−1785.

Scheme 2. Two Products of the Gas-Phase Hydrazinium/Acetone Reaction in the Presence of Neutral Hydrazine

Figure 1. SIFT-CIMS apparatus.
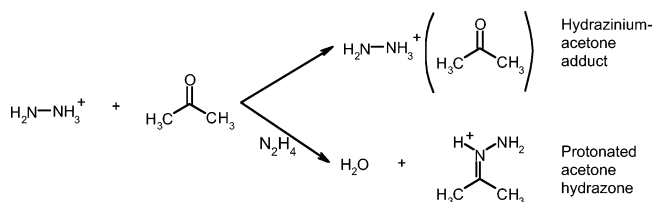
recently published a detailed work concerning unimolecular decomposition and collision-induced dissociation of protonated hydrazine adducts of the form $H^+(N_2H_4)_m(H_2O)_n$. Additional thermochemical information concerning bond strengths and heats of formation for $N_2H_5^+$ and related neutrals and radicals is given in Armstrong et al.[7] Gas-phase addition to carbonyl compounds has also been examined previously in a variety of contexts,[8–10] although never using hydrazinium or hydrazine as a nucleophile.
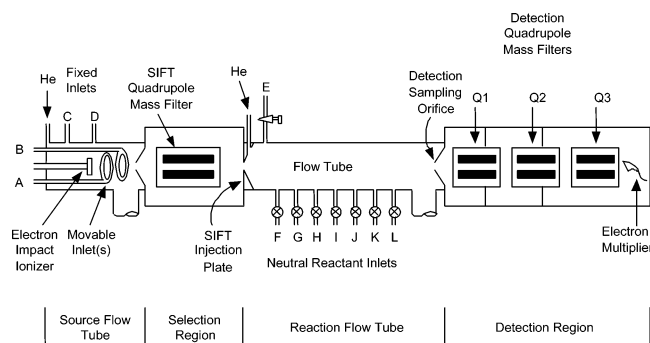
Recently, we reported that protonated hydrazone (or hydrazonium) formation is unique to carbonyl compounds in the gas-phase and that these reactions can be used to selectively quantify carbonyls in the atmosphere using chemical ionization mass spectrometry (CIMS) methods.[11,12] These experiments employed a flow-drift tube instrument operating near 1.4 Torr pressure and using drift fields of $20-35$ V cm^{-1}. These conditions are similar to those in instruments which have been developed specifically for on-line detection of trace species at levels as low as 10 ppt.[13] We found that hydrazinium reacts with carbonyl compounds in the presence of neutral hydrazine to form stable adducts and hydrazonium cations. For example, in the reaction of acetone with hydrazinium, two main products were detected: a protonated hydrazone and an adduct (Scheme 2), discussed in more detail later. Both adducts and hydrazonium are produced in high abundance with their ratio depending on the carbonyl structure and the strength of the applied drift field.

Clearly, the venerated solution chemistry of hydrazine shows promise when extended to gas-phase analytical chemistry. Thus, the present research was initiated to elucidate the reactive processes involved in hydrazonium formation for these studies and to provide a general framework for their formation under a variety of other gas-phase reaction conditions. To accomplish these goals, reactions between $N_2H_5^+$ and carbonyls were explored using a selected ion flow tube−chemical ionization mass spectrometer (SIFT-CIMS) and hybrid density functional theory calculations. No drift-field was employed for these experiments, and reaction region pressures were maintained at ~0.5 Torr.

Experimental Section

Materials. All compounds were obtained from Sigma-Aldrich with the exception of deuterated hydrazine (Isotec, Inc., min 98 atom %

D). He (>99.998%) was used as the buffer gas in the SIFT-CIMS and was passed through a liquid nitrogen-cooled molecular sieve trap prior to introduction into the instrument.

Experimental Overview. All experiments were performed using a selected ion flow tube−chemical ionization mass spectrometer (SIFT-CIMS) at the University of Colorado, Boulder, that has been described in detail previously.[14] Briefly, this instrument (Figure 1) consists of four sections: an ion source, an ion selection region, a reaction flow tube, and a detection system. A flowing afterglow ion source is used to produce ions, which are mass-selected using the ion selection region quadrupole mass filter and injected into the reaction flow tube. Ion/molecule reactions are examined by adding neutral reagents to the ions in the reaction region through any of several inlets. Ionic reaction products are analyzed and detected using a triple-quadrupole mass filter and an electron multiplier.

Ion Generation and Selection. Ionization is achieved by electron impact ionization in ~0.23 Torr He buffer gas. Addition of trace amounts of neutral precursors through inlets positioned at various distances along the ion source flow tube allowed formation of the reagent ions. Addition of H_2O results in formation of a mixture of $H_3O^+(H_2O)_n$ ($n = 0-3$) ions. Subsequent addition of N_2H_4 produces a mixture of $N_2H_5^+$ and $N_2H_5^+(N_2H_4)$, since H_3O^+ transfers a proton to N_2H_4. Addition of N_2H_4 alone also produces a mixture of $N_2H_5^+$ and $N_2H_5^+(N_2H_4)$, but the ion signal is not as large or as stable as when H_2O is added. Alternatively, addition of H_2O followed by a carbonyl, such as propanal, results in formation of a mixture of ions including $CH_3CH_2CHOH^+$ and $CH_3CH_2CHOH^+(CH_3CH_2CHO)$. Addition of N_2H_4 followed by a carbonyl (e.g. propanal) results in formation of $N_2H_5^+(CH_3CH_2CHO)$, $N_2H_5^+(N_2H_4)(CH_3CH_2CHO)$, $N_2H_5^+(CH_3CH_2CHO)_2$, and small amounts of $CH_3CH_2CH{=}HNNH_2^+$ and $CH_3CH_2CH{=}HNNH_2^+(N_2H_4)$.

Ion Reactions. Ions can be mass-selected and injected into the reaction flow tube using the SIFT quadrupole mass filter. Injected ions are entrained in a flow of helium and are reacted with neutral reagents added through inlets spaced over the length of the reaction flow tube (see E through L in Figure 1). For example, the hydrazinium/propanal adduct $N_2H_5^+(CH_3CH_2CHO)$ can be formed by injecting $N_2H_5^+$ into the reaction region followed by addition of CH_3CH_2CHO through inlet E (reaction 1).

$$N_2H_5^+ + CH_3CH_2CHO + He \rightarrow N_2H_5^+(CH_3CH_2CHO) + He \quad (1)$$

Addition of excess N_2H_4, simultaneously introduced through inlet F, brings about formation of the protonated hydrazone, $CH_3CH_2CH{=}HNNH_2^+$ (reaction 2).

$$N_2H_5^+(CH_3CH_2CHO) + N_2H_4 \rightarrow$$
$$CH_3CH_2CH{=}HNNH_2^+ + H_2O + N_2H_4 \quad (2)$$

(7) Armstrong, D. A.; Yu, D.; Rauk, A. *J. Phys. Chem. A* **1997**, *101*, 4761−4769.

(8) Born, M.; Ingemann, S.; Nibbering, N. M. M. *Mass Spectrom. Rev.* **1997**, *16*, 181−200.

(9) Bache-Andreassen, L.; Uggerud, E. *Org. Biomol. Chem.* **2003**, *1*, 705−713.

(10) Nixdorf, A.; Grutzmacher, H.-F. *Int. J. Mass Spectrom.* **2000**, *195/196*, 533−544.

(11) Morrison, G. C.; Howard, C. J. *Int. J. Mass Spectrom.* **2001**, *210/211*, 503−509.

(12) Morrison, G. C.; Howard, C. J. *Proc. 94th Annu. Meet. Air Waste Manage. Assoc.* **2001**, paper 165; Air & Waste Management Association: Pittsburgh.

(13) Lindinger, W.; Hansel, A.; Jordan, A. *Int. J. Mass Spectrom. Ion Processes* **1998**, *173*, 191−241.
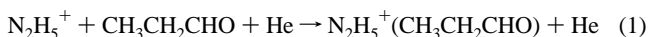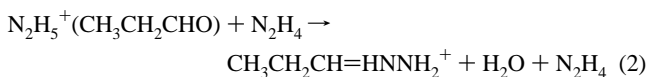
(14) Van Doren, J. M.; Barlow, S. E.; DePuy, C. H.; Bierbaum, V. M. *Int. J. Mass Spectrom. Ion Processes* **1987**, *81*, 85−100.

Table 1. Summary of Experimental Configurations

	summary of reactions tested for this study					
	ion source			reaction region		
experiment	inlet A	inlet B	mass selected/injected, *m/z*	inlet E	inlet F	inlet L
1	H_2O	N_2H_4	33 $N_2H_5^+$	carbonyl	−	−
2	H_2O	N_2H_4	33 $N_2H_5^+$	propanal	N_2H_4	−
3	N_2H_4	propanal	91 $N_2H_5^+(CH_3CH_2CHO)$	−	N_2H_4	−
4	H_2O	N_2H_4	65 $N_2H_5^+(N_2H_4)$	−	−	−
5	H_2O	N_2H_4	65 $N_2H_5^+(N_2H_4)$	propanal	−	−
6	H_2O	N_2H_4	65 $N_2H_5^+(N_2H_4)$	acetone	−	−
7	H_2O	propanal	59 $CH_3CH_2CHOH^+$	−	N_2H_4	−
8	H_2O	acetone	59 $(CH_3)_2C(O)H^+$	−	N_2H_4	−
9	H_2O	N_2H_4	33 $N_2H_5^+$	−	N_2D_4	−
10	H_2O	N_2H_4	33 $N_2H_5^+$	butanal	−	N_2D_4
11	H_2O	N_2H_4	33 $N_2H_5^+$	butanal	N_2D_4	−
12	H_2O	N_2H_4	33 $N_2H_5^+$	acetaldehyde	H_2O	−
13	H_2O	N_2H_4	33 $N_2H_5^+$	acetone	H_2O	−
14	H_2O	N_2H_4	33 $N_2H_5^+$	formaldehyde	H_2O	−

Alternatively, similar adducts and hydrazones can be generated directly in the source flow tube by adding both N_2H_4 and CH_3CH_2CHO. Mass selection and injection of the $N_2H_5^+(N_2H_4)(CH_3CH_2CHO)$ or $CH_3CH_2CH=HNNH_2^+$ ions produces detectable signals of the hydrazonium, $CH_3CH_2CH=HNNH_2^+$, in the reaction flow tube. Table 1 gives a summary of the experimental configurations employed in this study.

Reaction Kinetics. We measured effective second-order rate coefficients for the association reactions of hydrazinium (e.g., reaction 1) and several neutral compounds at a helium pressure of 0.5 Torr and a temperature of 300 K. The compounds studied include C_1 through C_6 aldehydes and ketones (acrolein, methacrolein, benzaldehyde, hexanal, acetone, butanone, and cyclopentanone) as well as three noncarbonyl compounds (benzene, ethanol, and heptane). A measured flow of the neutral compound was added through each of the inlet ports in random order while the depletion of injected $N_2H_5^+$ was measured (experiment 1, Table 1). The rate coefficient for the reaction of $N_2H_5^+(CH_3CH_2CHO)$ with N_2H_4 to form protonated hydrazone was also measured (experiment 3, Table 1).

Determination of second-order rate coefficients in ion flow tubes has been described elsewhere.[15] Briefly, the pseudo-first-order kinetics for reaction of the reagent ion, A^+, with a large excess of neutral analyte species, B, is described by:

$$\ln[A^+]_0 - \ln[A^+] = k[B]t \qquad (3)$$

where $[A^+]_0$ is the initial reagent ion concentration, $[A^+]$ is the reagent ion concentration in the presence of reactant B, k is the reaction rate coefficient, and t is the mean ion−neutral reaction time.

Hybrid Density Functional Theory Calculations. Hybrid density functional theory calculations were performed using the Gaussian 98 program[16] with the goal of obtaining thermochemical and structural information for each step in the gas-phase reaction between hydrazinium ($N_2H_5^+$) and a carbonyl. Geometries were optimized using B3LYP density functional theory[17−19] and the 6-31G(d) basis set. Harmonic frequencies were calculated using analytical gradient procedures and

were utilized to identify stationary points as either minima on the potential surface (no imaginary frequency) or transition states (exactly one imaginary frequency). Zero point vibrational energies (ZPE) were also obtained from the frequency analysis and scaled by an empirical factor of 0.9806[20] prior to correction of the electronic energy. Intrinsic reaction coordinate calculations[21,22] were performed in the forward and reverse directions to establish which minima were connected by a given transition state. Single point energies were calculated at the previously optimized geometries using the expanded 6-311+G(2d, 2p) basis set and corrected for zero point energies determined using the smaller basis set.

Proton affinities of hydrazine (N_2H_4), ammonia (NH_3), formaldehyde (CH_2O), acetaldehyde (CH_3CHO), propanal (CH_3CH_2CHO), acetone ($(CH_3)_2CO$), butanal ($CH_3CH_2CH_2CHO$), and butanone ($CH_3CH_2C(O)CH_3$) were computed (see Supporting Information). Good agreement is obtained between results of calculations using the expanded basis set and literature values,[23] with the deviation being typically less than 5 kJ mol^{-1}. Additional comparisons between calculation and experiment can be made for the enthalpy of association of $N_2H_5^+$ with N_2H_4. The calculated value is 107 kJ mol^{-1}, which is in reasonable agreement with the experiments of Feng et al.[6] who report a binding energy of 135 kJ mol^{-1} as well as with compiled experimental enthalpies of association for similar ions and molecules listed in Keesee and Castleman[24] (ΔH is ~132 kJ mol^{-1} for H_3O^+ clustering with H_2O or ~104 kJ mol^{-1} for NH_4^+ clustering with NH_3). G2 calculations for the reaction between hydrazinium and formaldehyde (provided in the Supporting Information) are also in reasonable agreement with those obtained using density functional theory. These results support the validity of our approach for the reactions under study.

Results

Mechanistic Studies. Experiments 1 through 14, shown in Table 1, were designed to determine the roles of $N_2H_5^+$ and N_2H_4 in the formation of hydrazonium products. Experiment 1 explores the products of the reaction of $N_2H_5^+$ with carbonyl species. Upon injection of $N_2H_5^+$, we observe formation of a small amount of NH_3^+(Figure 2a). This product is also observed by Oiestad and Uggerud.[5] Addition of a carbonyl (e.g., propanal)

(15) Van Doren, J. M. Ph.D. Thesis, University of Colorado at Boulder, 1987.
(16) Frisch, M. J.; Trucks, G. W.; Schlegel, H. B.; Scuseria, G. E.; Robb, M. A.; Cheeseman, J. R.; Zakrzewski, V. G.; Montgomery, J. A. J.; Stratmann, R. E.; Burant, J. C.; Dapprich, S.; Millam, J. M.; Daniels, A. D.; Kudin, K. N.; Strain, M. C.; Farkas, O.; Tomasi, J.; Barone, V.; Cossi, M.; Cammi, R.; Mennucci, B.; Pomelli, C.; Adamo, C.; Clifford, S.; Ochterski, J.; Petersson, G. A.; Ayala, P. Y.; Cui, Q.; Morokuma, K.; Malick, D. K.; Rabuck, A. D.; Raghavachari, K.; Foresman, J. B.; Cioslowski, J.; Ortiz, J. V.; Stefanov, B. B.; Liu, G.; Liashenko, A.; Piskorz, P.; Komaromi, I.; Gomperts, R.; Martin, R. L.; Fox, D. J.; Keith, T.; Al-Laham, M. A.; Peng, C. Y.; Nanayakkara, A.; Gonzalez, C.; Challacombe, M.; Gill, P. M. W.; Johnson, B.; Chen, W.; Wong, M. W.; Andres, J. L.; Gonzalez, C.; Head-Gordon, M.; Replogle, E. S.; Pople, J. A. Gaussian 98, Revision A.6 ed.; Gaussian, Inc.: Pittsburgh, PA, 1998.

(17) Lee, C.; Yang, W.; Parr, R. G. *Phys. Rev. B* **1988**, *37*, 785−789.
(18) Miehlich, B.; Savin, A.; Stoll, H.; Preuss, H. *Chem. Phys. Lett.* **1989**, *157*, 200−206.
(19) Becke, A. D. *J. Chem. Phys.* **1993**, *98*, 5648−5652.
(20) Scott, A. P.; Radom, L. *J. Phys. Chem.* **1996**, *100*, 16502−16513.
(21) Gonzalez, C.; Schlegel, H. B. *J. Chem. Phys.* **1989**, *90*, 2154−2161.
(22) Gonzalez, C.; Schlegel, H. B. *J. Phys. Chem.* **1990**, *94*, 5523−5527.
(23) Hunter, E. P. L.; Lias, S. G. *J. Phys. Chem. Ref. Data* **1998**, *27*, 413−656.
(24) Keesee, R. G.; Castleman, A. W., Jr. *J. Phys. Chem. Ref. Data* **1986**, *15*, 1011−1071.
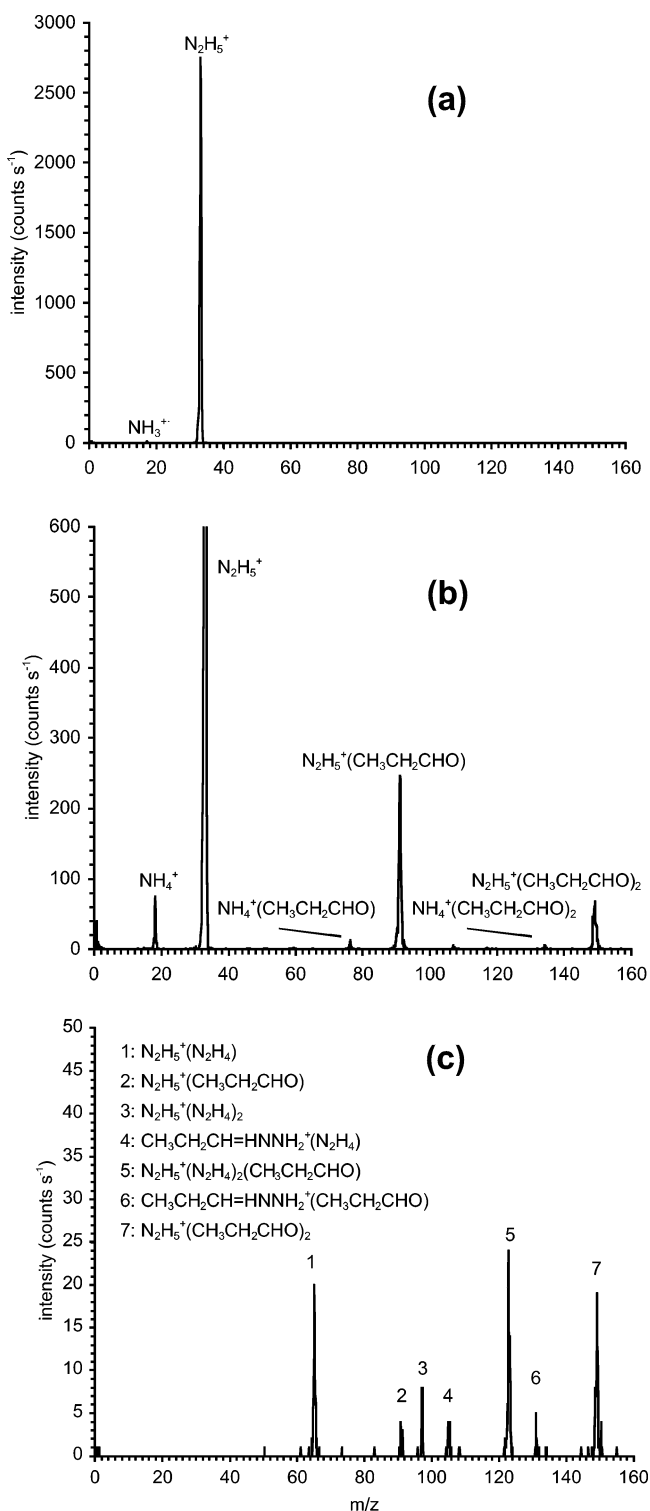
Figure 2. $N_2H_5^+$ association with propanal. (a) Some fragmentation to NH_3^+ occurs upon injection of $N_2H_5^+$. (b) Addition of propanal to the flow tube produces the $N_2H_5^+(CH_3CH_2CHO)$ adduct and the $N_2H_5^+(CH_3CH_2CHO)_2$ adduct. NH_4^+ also forms and clusters with propanal. No hydrazone products are formed. (c) Addition of N_2H_4 to the flow tube results in hydrazone formation, $CH_3CH_2CH=HNNH_2^+$.

forms the adducts $N_2H_5^+(propanal)$ and $N_2H_5^+(propanal)_2$ (Figure 2b). Since these latter reactions do not interfere with studies of protonated hydrazone formation, they will not be discussed further except as Supporting Information. A key finding from this experiment is that no hydrazone forms under these conditions.

Experiments 2 and 3 were performed to determine if neutral hydrazine is necessary for the formation of the hydrazonium. In experiment 2, the reaction of $N_2H_5^+$ with excess propanal added through inlet E produces the association product, $N_2H_5^+(CH_3CH_2CHO)$, and completely depletes $N_2H_5^+$. Neutral hydrazine is then introduced at inlet F. Protonated propanal hydrazonium clustered with hydrazine, $CH_3CH_2CH=HNNH_2^+-(N_2H_4)$, is detected as a product of the reaction between the association product, $N_2H_5^+(CH_3CH_2CHO)$, and hydrazine, N_2H_4 (Figure 2c). To clearly demonstrate this sequence, in experiment 3, the association product $N_2H_5^+(CH_3CH_2CHO)$ is mass-selected and injected into the reaction flow tube, and neutral hydrazine is added at inlet F. The results of experiment 3 are nearly identical to those of experiment 2. In similar tests, it was found that acetone does not produce hydrazonium as readily as propanal under the conditions of experiment 2. This result can be contrasted with observation of acetone hydrazonium formation in previous studies[11,12] where a drift field is employed. The results of experiments 1, 2, and 3 indicate that both $N_2H_5^+$ and N_2H_4 are required to form the hydrazonium from a carbonyl at thermal energies.

Experiments 4−6 were designed to determine if the reaction of the adduct $N_2H_5^+(N_2H_4)$ with carbonyls would also produce hydrazones. The process of injecting $N_2H_5^+(N_2H_4)$ breaks up many of these adducts, forming $N_2H_5^+$ (experiment 4, Figure 3a). Addition of propanal to the flow tube allows reaction with $N_2H_5^+(N_2H_4)$ to form a small amount of hydrazonium, $CH_3CH_2CH=HNNH_2^+(N_2H_4)$ (experiment 5, Figure 3b). However, the comparable reaction with acetone does not produce a hydrazonium (experiment 6). These experiments show that neutral hydrazine plays a role in hydrazonium formation at thermal energies and that hydrazine is more effective in producing a hydrazonium from propanal than from acetone.

A series of tests were conducted to examine the reactions of protonated carbonyls with hydrazine. In experiments 7 and 8, protonated propanal and protonated acetone were mass selected and injected into the reaction flow tube. Figure 4a shows the result of injecting protonated propanal with partial fragmentation to form $m/z = 31$ (possibly H_2COH^+). Both protonated carbonyls react rapidly with N_2H_4 introduced at inlet F (Figure 4b). With propanal, a small amount of hydrazonium product is formed but no hydrazonium is observed in the case of acetone. The primary product from both reactions is $N_2H_5^+$ resulting from proton transfer. This reaction occurs because the proton affinity of hydrazine is 70 and 39 kJ mol^{-1} higher than propanal and acetone, respectively.[23] These experiments show that the charged species need not be $N_2H_5^+$ for a hydrazonium to form in the aldehyde reaction.

In experiments 9−11, we used deuterated hydrazine to explore the mechanisms of these reactions. N_2D_4 is added to the flow tube with $N_2H_5^+$ in experiment 9. The interaction of these species results in complete H/D scrambling, and every permutation of $N_2H_nD_{5-n}^+$ ($n = 0$ to 5) is observed along with various adducts (e.g., $N_2H_4D^+(N_2D_4)$, $N_2H_3D_2^+(N_2D_4)$, etc.). The rapid scrambling of deuterium shows that care must be taken when interpreting the products of deuterated hydrazine reactions.

Experiments 10 and 11 are similar to experiment 2, except that butanal is the carbonyl species and perdeuteriohydrazine, N_2D_4, is added after addition of the carbonyl. $N_2H_5^+$ is injected
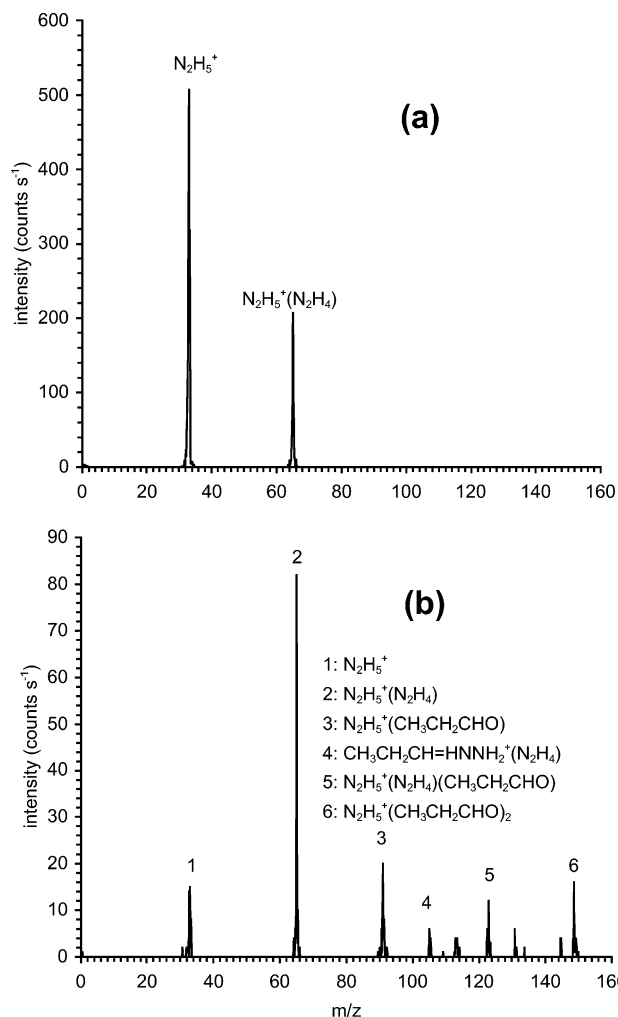
Figure 3. Hydrazone formation by the reaction of propanal with the adduct $N_2H_5^+(N_2H_4)$. (a) Some fragmentation to $N_2H_5^+$ occurs upon injection of $N_2H_5^+(N_2H_4)$ (b) The protonated propanal hydrazone clustered with hydrazine, $CH_3CH_2CH{=}HNNH_2^+(N_2H_4)$, forms following addition of propanal to the flow tube.

Figure 4. Hydrazone formation by the reaction of hydrazine with protonated propanal, $CH_3CH_2CHOH^+$. (a) Some fragmentation to H_2COH^+ occurs upon injection of $CH_3CH_2CHOH^+$. (b) Small amounts of $CH_3CH_2CH{=}HNNH_2^+$ and $CH_3CH_2CH{=}HNNH_2^+(N_2H_4)$ form following addition of N_2H_4 to the flow tube. Primarily, protons are abstracted from $CH_3CH_2CHOH^+$ by N_2H_4 due to the higher proton affinity of hydrazine.

into the reaction region and, immediately after the injection plate, butanal is introduced at inlet E. These reactants form adducts, which include $N_2H_5^+(CH_3CH_2CH_2CHO)$. A sufficiently high flow of butanal is added to quantitatively convert $N_2H_5^+$ to $N_2H_5^+(CH_3CH_2CH_2CHO)$ prior to inlet F. This adduct is then reacted with N_2D_4 (introduced at inlet F or L) to form a hydrazonium product. If N_2D_4 is involved in C−N bond formation, a fully N-deuterated hydrazonium ion should be produced as a product (e.g. $CH_3CH_2CH_2CH{=}DNND_2^+$). This deuterated hydrazonium may lose deuterium by subsequent H/D exchange with butanal, $CH_3CH_2CH_2CHO$. In analogy with previously proposed H/D exchange mechanisms,[25] only labile deuterons can be exchanged for protons, and therefore all three deuterons connected to N atoms may be exchanged.

When the N_2D_4 concentration is low and the reaction time is short (∼0.001 s, obtained by addition of reactant through inlet L, experiment 10), only one product is detected: CH_3CH_2-$CH_2CH{=}DNND_2^+$ ($m/z = 90$). Few collisions occur between this deuterated hydrazonium cation and butanal prior to sampling into the detection region. This largely prevents both adduct formation and H/D exchange. This result also rules out isotope
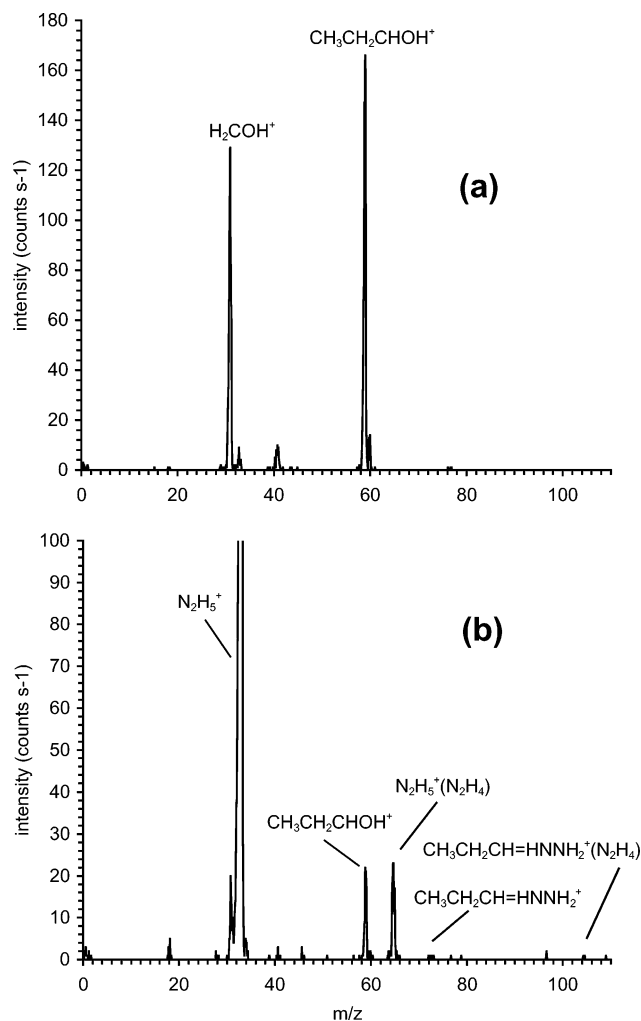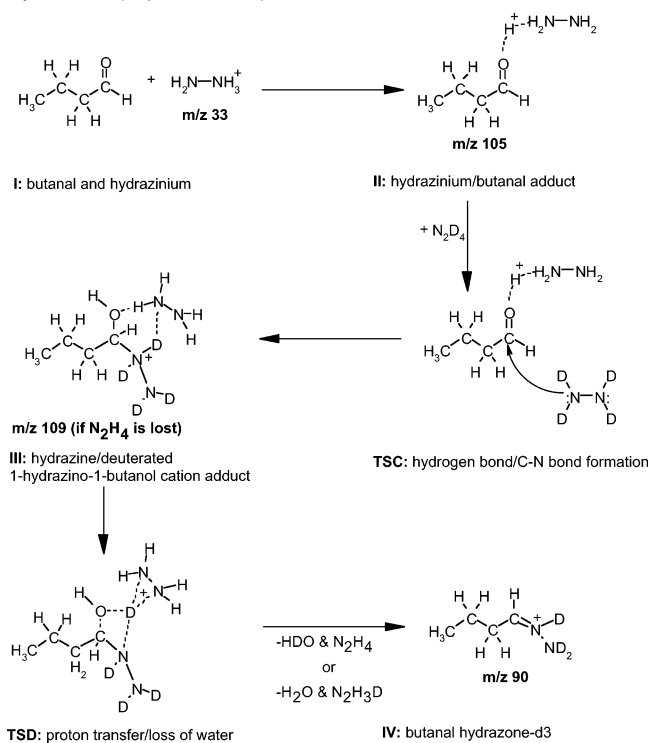
(25) Hunt, D. F.; Sethi, S. K. *J. Am. Chem. Soc.* **1980**, *102*, 6953−6963.

scrambling between $N_2H_5^+$ and N_2D_4 within the termolecular intermediate (i.e., the species formed immediately following collision of $N_2H_5^+(CH_3CH_2CH_2CHO)$ with N_2D_4) which might otherwise yield isotopic variants of the hydrazonium cation without the need for subsequent collisions with butanal. When N_2D_4 is added early in the reaction region, the residence time of the deuterated hydrazonium cation in the flow tube is substantial (∼0.006 s, obtained by addition through inlet F, experiment 11). Many collisions occur between the deuterated hydrazonium and butanal, and a range of scrambled hydrazone products are detected along with adducts. Full exchange of three hydrogens was observed for experiment 11, indicating the labile H atoms are located on the N atoms.

The observation of the N-deuterated hydrazonium cation, $CH_3CH_2CH_2CH{=}DNND_2^+$, is the major result from this set of experiments as this species confirms the role of neutral hydrazine in hydrazone formation. Scheme 3 presents the proposed gas-phase mechanism for its formation. Butanal-hydrazone formation begins with the association of butanal and hydrazinium (I), to form the adduct (II). The carbonyl carbon of the adduct is rendered vulnerable to attack by the lone electron pair of

Scheme 3. Proposed Mechanism for the Formation of Butanal Hydrazone (experiment 10)[a]

I: butanal and hydrazinium

II: hydrazinium/butanal adduct

m/z 109 (if N_2H_4 is lost)

III: hydrazine/deuterated 1-hydrazino-1-butanol cation adduct

TSC: hydrogen bond/C−N bond formation

TSD: proton transfer/loss of water

-HDO & N_2H_4
or
-H_2O & N_2H_3D

IV: butanal hydrazone-d3

m/z 90

[a] Loss of HDO and N_2H_4 or loss of H_2O and N_2H_3D may be expected depending on the nature of TSC. See Scheme 6 and discussion for details. Labels reflect those used for Figures 5a and 5b. "TS" indicates a transition state.

deuterated hydrazine due to interaction with the hydrazinium proton. Hydrogen and C−N bond formation begins (TSC, where "TS" indicates a transition state). The result is deuterated 1-hydrazino-1-butanol cation clustered with neutral N_2H_4 (III). Neutral N_2H_4 is lost and an ion at m/z 109 formed, or neutral N_2H_4 remains to facilitate transfer of a deuteron from the nitrogen atom (α to the carbonyl carbon) to the carbonyl oxygen or to the remaining N_2H_4 molecule. Transfer of a deuteron onto either of these species (TSD) occurs, through either a concerted or stepwise process to form the observed butanal hydrazone-d_3 at m/z 90 (IV). The concerted process is pictured in Scheme 3. As a consequence of hydrazone formation, a combination of either N_2H_4 and HDO or N_2H_3D and H_2O will be released. An identical scheme can be written replacing N_2D_4 with N_2H_4.

Experiments 12−14 were designed to explore the possible role of ligand switching[26,27] in the hydrazine chemistry, since high concentrations of H_2O are often present in CIMS applications.

$$N_2H_5^+(\text{carbonyl}) + H_2O \rightleftharpoons N_2H_5^+(H_2O) + \text{carbonyl} \quad (4)$$
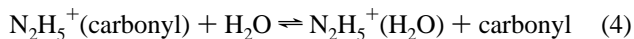
To examine the effect of ligand switching with water (reaction 4), a large concentration of the carbonyl was added to the flow tube to completely deplete the injected $N_2H_5^+$, thus forming the carbonyl-hydrazinium adduct, $N_2H_5^+$(carbonyl). Water was then added at Inlet F. The $N_2H_5^+(H_2CO)$ adduct is rapidly destroyed by water whereas there is no significant ligand switching

(26) Adams, N. G.; Bohme, D. K.; Dunkin, D. B.; Fehsenfeld, F. C.; Ferguson, E. E. *J. Chem. Phys.* **1970**, *52*, 3133−3140.
(27) Hansel, A.; Singer, W.; Wisthaler, A.; Schwarzmann, M.; Lindinger, W. *Int. J. Mass Spectrom. Ion Processes* **1997**, *167/168*, 697−703.

Table 2. Second-Order Rate Coefficients Measured for the Association Reaction of $N_2H_5^+$

compound	measured rate coefficient[a] (10^{-9} cm³ s⁻¹)	reaction efficiency ($k_{measd}/k_{calcd}) \times 100$
formaldehyde	0.019 ± 0.002	0.66
acetaldehyde	0.28 ± 0.04	8.8
propanal	0.8 ± 0.1	27
acrolein	0.7 ± 0.1	20
butanal	1.4 ± 0.2	44
methacrolein	1.2 ± 0.2	−
pentanal	1.8 ± 0.3	58
hexanal	2.0 ± 0.5	67
benzaldehyde	2.5 ± 0.4	83
acetone	1.3 ± 0.2	39
butanone	1.8 ± 0.3	56
cyclopentanone	2.1 ± 0.3	−
benzene	0.13 ± 0.01	8.1
ethanol	0.24 ± 0.03	10
heptane	<0.001	<0.06

[a] He pressure 0.5 Torr and temperature of 300 K. [b] Values calculated based on dipole moments and polarizabilities estimated by Spanel et al. (reference 35). All others calculated using values from Lide (ref 36).

reactions between $N_2H_5^+(CH_3CHO)$ or $N_2H_5^+((CH_3)_2CO)$ and water. These results suggest that the presence of water will not preclude hydrazone formation for most carbonyl compounds.

Reaction Kinetics. The effective second-order rate coefficients for adduct formation reactions of $N_2H_5^+$ are shown in Table 2 as well as the reaction efficiencies (where collisional rate coefficients were calculated based on the method of Su and Chesnavich[28]). Most measured rate coefficients are of the order of 10^{-9} cm³ molecule⁻¹ s⁻¹. However, the rate coefficients and reaction efficiencies for formaldehyde and acetaldehyde are much lower than for the other carbonyls. The measured rate coefficients increase with molecular weight and size of the reacting carbonyl. The largest carbonyls studied, hexanal and benzaldehyde, have the largest measured rate coefficients, which were 67 and 83%, respectively, of the calculated collisional rate coefficients. Noncarbonyl species react more slowly. Benzene and ethanol react with rate coefficients comparable to that of acetaldehyde and there was no detectable reaction with heptane.
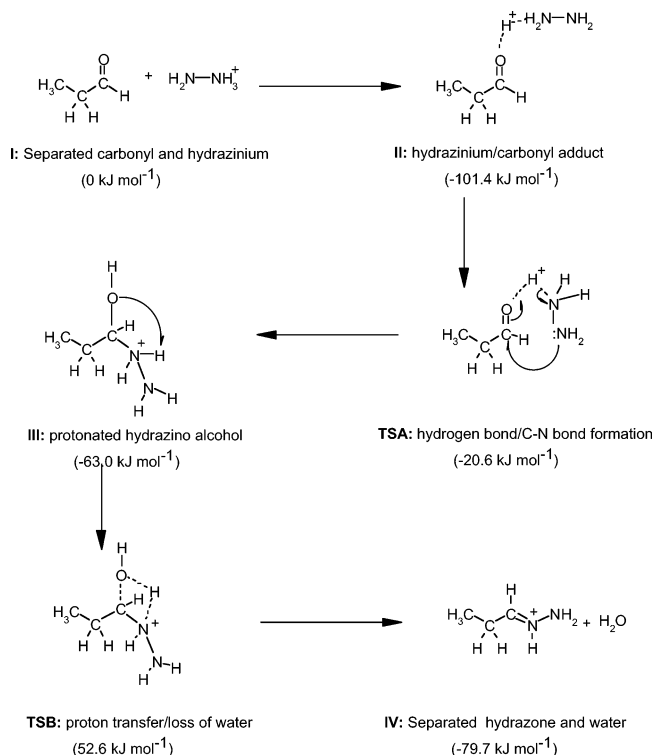
According to Scheme 3, the hydrazinium−carbonyl adduct must react with neutral hydrazine in order to produce protonated hydrazone. To determine if this second step is rate limiting in the formation of the hydrazone, we measured the second-order rate coefficient for the reaction of the adduct, $N_2H_5^+(CH_3CH_2-CHO)$, with N_2H_4 and determined a value of 2.2×10^{-9} cm³ molecule⁻¹ s⁻¹. Observable products include $CH_3CH_2CH=HNNH_2^+$ and $CH_3CH_2CH=HNNH_2^+(N_2H_4)$, which account for only about 8% of the initial parent ion concentration. The other 92% of the parent ion loss can reasonably be attributed to ligand switching (e.g., N_2H_4 replacing the carbonyl of the $N_2H_5^+$(carbonyl) adduct) which is calculated to be exothermic by ~26 kJ mol⁻¹ (also see Supporting Information). Evidence of this reaction will be obscured by the simultaneous formation of $N_2H_5^+(N_2H_4)$ from the reaction between $N_2H_5^+$ and N_2H_4. Assuming the observed product yield accurately reflects the kinetics, we can reasonably partition the observed overall rate coefficient according to the percent abundance of products to obtain a lower limit for the rate coefficient for hydrazone formation: ~0.2×10^{-9} cm³ molecule⁻¹ s⁻¹. This is somewhat smaller than the rate coefficient for the formation of the adduct,

(28) Su, T.; Chesnavich, W. J. *J. Chem. Phys.* **1982**, *76*, 5183−5185.

Scheme 4. Possible Reaction Mechanism that Forms a Protonated Hydrazone Directly from $N_2H_5^+$ Attack on Propanal[a]

I: Separated carbonyl and hydrazinium
(0 kJ mol^{-1})

II: hydrazinium/carbonyl adduct
(-101.4 kJ mol^{-1})

III: protonated hydrazino alcohol
(-63.0 kJ mol^{-1})

TSA: hydrogen bond/C-N bond formation
(-20.6 kJ mol^{-1})

TSB: proton transfer/loss of water
(52.6 kJ mol^{-1})

IV: Separated hydrazone and water
(-79.7 kJ mol^{-1})

[a] This process is found to have a large energy barrier and does not occur at thermal energies. Labels and energies reflect those used for Figures 5a and 5b. "TS" indicates a transition state.

$N_2H_5^+(CH_3CH_2CHO)$ (0.8×10^{-9}, Table 2), but is still only 1 order of magnitude less than a collisional rate coefficient. This estimate suggests that hydrazonium formation, and not adduct formation, is rate limiting at thermal energies.

Hybrid Density Functional Calculations. The reactions of $N_2H_5^+$ with acetone and propanal were chosen as model systems for calculations, since most of the accompanying experimental data involved these species. The experimental observations, specifically that the hydrazonium is not formed directly from the reaction between $N_2H_5^+$ and a carbonyl and that reactions involving propanal adducts have a greater propensity to form hydrazonium than those involving acetone adducts, provide distinctions that were examined with calculations. The first mechanism explored is represented in Scheme 4. This scheme describes a possible mechanism for the direct reaction of $N_2H_5^+$ and propanal forming protonated hydrazone, a process not observed in our experiments. This process is directly analogous to the reactions of experiment 1, where $N_2H_5^+$ is reacted with a carbonyl without subsequent addition of neutral hydrazine. Insight into the results of experiments 7 and 8, where protonated acetone and propanal are reacted with neutral hydrazine, can also be obtained. Such calculations help elucidate the steps in hydrazone formation and serve as a starting point for our further inquiry into transition states and structures that include an additional molecule of neutral hydrazine.

Results of calculations are plotted in Figures 5a and 5b for the hydrazinium ion interactions with propanal and acetone, respectively. Z-matrices, energies, and structures are given as Supporting Information. Also shown on the left of these figures are the energies of the reactants of experiments 7 and 8:

$CH_3CH_2CHOH^+/N_2H_4$ and $(CH_3)_2COH^+/N_2H_4$. All energies are plotted with respect to the sum of the energies of the separated reactants.

Although not pictured, numerous minima were found for structures III and IV. More than five minima for III were found with various degrees of rotation about the C–N, the N–N, and the C–O bonds. Many more structures are likely to exist. These conformations are within 10 kJ mol^{-1} of one another, and it is assumed that interconversion among them will occur easily under the thermal energy reaction conditions of the SIFT-CIMS instrument. Although a proton can be transferred between the two N atoms of III to facilitate the loss of water and formation of IV, the barrier to such interconversion is quite high (~180 kJ mol^{-1}). This is in good agreement with energies obtained previously for transfer of a proton from one nitrogen to another in $N_2H_5^+$ where values of 184 kJ mol^{-1} and 186.6 kJ mol^{-1} were reported.[5,29] Such proton transfer should be a rare occurrence for thermalized ions. In a similar way, the barrier to transfer of a proton across N atoms of protonated formaldehyde–hydrazonium cations (e.g., structures such as IV) was reported to be ~220 kJ mol^{-1}.[30] Since, for hydrazonium (IV), it is more energetically favorable (~28 to 48 kJ mol^{-1}) for a proton to reside on the N atom of the C=N double bond rather than on the terminal N atom, it is assumed that this is the species observed during experiments. Syn/anti isomers of asymmetric hydrazones have been observed previously and are thought to interconvert with a barrier of ~145 kJ mol^{-1} for neutral hydrazone molecules.[31] Similarly, interconversion is unlikely for thermalized ions in the SIFT-CIMS instrument. Differences in energies calculated between the syn and anti hydrazonium ions of propanal amount to less than 1 kJ mol^{-1}, and it is unlikely that either the syn or anti form will be strongly favored in the gas phase.
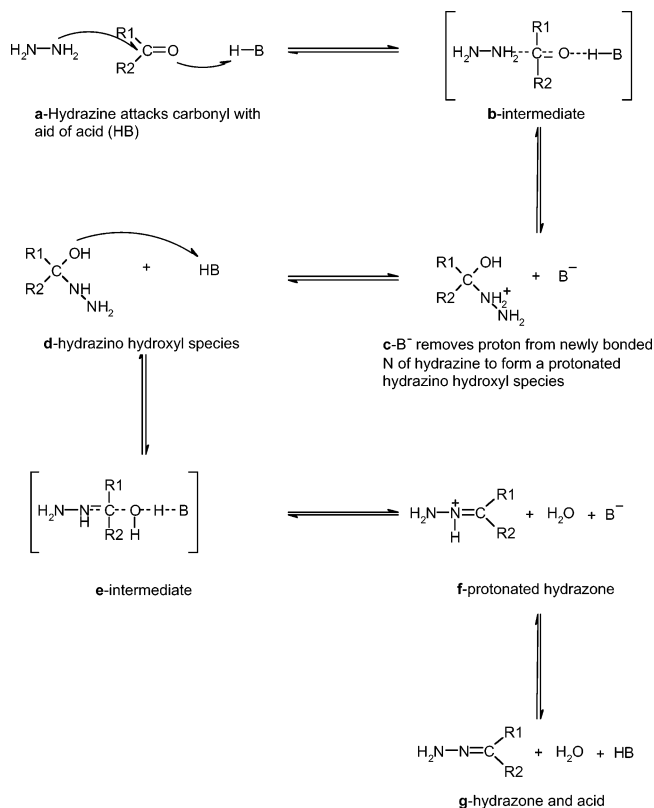
Discussion

These studies explore a number of reactive processes leading up to or competing with hydrazonium formation and also reveal complexities associated with the mechanism of hydrazonium formation. Association reactions and switching reactions are the main processes that may give rise to or compete with eventual hydrazone formation. Experiments and calculations provide insight into the mechanism of hydrazonium formation for the two-body ion–molecule reaction processes (Scheme 4). Experiments provide further insight when a third reactive molecule, namely N_2H_4 or N_2D_4 in Scheme 3, is subsequently involved. Both our results and results of previous studies suggest a role for chemical or translational activation in hydrazone formation. The discussion below considers these reactions in detail and should aid in understanding experiments employing hydrazinium as a CIMS reagent for trace gas detection.[11,12]

Adduct Formation. At thermal energies, the formation of an adduct is the first step in hydrazone formation. The observation that the $N_2H_5^+(carbonyl)$ adduct formation rate coefficients at 0.5 Torr and 300 K increase with molecular weight suggests that these measurements were made in the "pressure dependent" regime[32,33] for compounds up to ~C5.

(29) Del Bene, J. E.; Frisch, M. J.; Raghavachari, K.; Pople, J. A. *J. Phys. Chem.* **1982**, *86*, 1529–1535.
(30) van Garderen, H. F.; Ruttink, P. J. A.; Burgers, P. C.; McGibbon, G. A.; Terlouw, J. K. *Int. J. Mass Spectrom Ion Processes* **1992**, *121*, 159–182.
(31) Benassi, R.; Taddei, F. *J. Chem. Soc., Perkin Trans. 2* **1985**, 1629–1632.

Scheme 5. Solution-Phase, Acid-Catalyzed Mechanism for Hydrazone Formation Taken from Ref 1

a-Hydrazine attacks carbonyl with aid of acid (HB)

b-intermediate

d-hydrazino hydroxyl species

c-B⁻ removes proton from newly bonded N of hydrazine to form a protonated hydrazino hydroxyl species

e-intermediate

f-protonated hydrazone

g-hydrazone and acid

Rate coefficients for larger compounds, e.g. benzaldehyde, approach the collision rate coefficient, the theoretical maximum. Many organic compounds, not just carbonyls, may associate with hydrazinium cation efficiently depending on ion−dipole interactions and molecular complexity. Carbonyl specific hydrazone formation is a separate process that follows adduct formation at thermal energies.

Hydrazone Formation. The requirement for both $N_2H_5^+$ and N_2H_4 molecules in the gas-phase formation of hydrazones at thermal energies deserves discussion. Although our experiments clearly demonstrate the mechanism, the complexity of the key intermediate, $N_2H_5^+$(carbonyl)(N_2H_4), made it impractical to carry out the computations needed to explore the reaction surface. The proposed mechanism for hydrazone formation in the gas-phase (Scheme 3) is similar to the aqueous solution mechanism (Scheme 5) adapted from the text of Sollenberger and Martin.[1] In solution, the free electron pair on hydrazine attacks the carbonyl carbon while the hydrogen of the acid interacts with the carbonyl oxygen. In the gas-phase, $N_2H_5^+$ acts as the acid and interacts with the carbonyl oxygen while neutral hydrazine acts as a nucleophile, attacking the carbonyl carbon. One proton from the newly bonded hydrazine must then be transferred to H_2O or N_2H_4 which are liberated in the final step of hydrazonium formation.

a. Bimolecular Processes. Our experimental results show that a hydrazonium is not formed in the gas-phase reaction of $N_2H_5^+$ with carbonyls at thermal energies (experiment 1, Scheme 4), but it seems to form via the termolecular mechanism

in Scheme 3. To understand this result, we turn to hybrid density functional calculations for the mechanism in Scheme 4, the results of which are given in Figures 5a and 5b. Transition states TSA and TSB involve formation of a C−N bond through nucleophilic attack and loss of water to form a hydrazonium product, respectively. Interestingly, C−N bond formation and loss of water have previously been invoked to explain the pH dependence of hydrazone formation in solution.[1] At low pH, attack by the nitrogen lone pair is impeded (TSA) by the tendency for the N_2H_4 to be converted to $N_2H_5^+$. At higher pH, carbonyl protonation and loss of water is hindered (TSB).

Calculations indicate that loss of water (TSB) presents the largest energetic barrier to hydrazone formation. Traversal of this barrier is therefore key to experimental observation of hydrazones. If we examine the proton affinity of the nitrogen (α to the carbonyl) of deprotonated analogues of III, this is quite reasonable. The calculated proton affinity of both 1-hydrazino-1-propanol and 2-hydrazino-2-propanol are approximately 910 and 913 kJ mol^{-1}, respectively. Similarly, 1-amino-1-propanol and 2-amino-2-propanol have proton affinities of approximatly 900 and 908 kJ mol^{-1}. The proton affinities of most non-nitrogen-containing alcohols (typically around ∼750−800 kJ mol^{-1} [23]) are much lower. In addition to being endothermic, intramolecular transfer of a proton from the nitrogen of structure III to the oxygen must also proceed through the highly strained four-membered ring of TSB (Scheme 4).

There is experimental evidence that TSB is positioned correctly relative to reactants in both Figures 5a and 5b. No hydrazonium formation is observed during experiments involving the reactants $CH_3CH_2CHO/N_2H_5^+$ and $(CH_3)_2CO/N_2H_5^+$ (I, Figures 5a and 5b). Examining experiments 7 and 8, the formation of a hydrazone is observed when protonated propanal is a reactant (e.g., $CH_3CH_2CHOH^+$ reacting with N_2H_4) but not when protonated acetone is a reactant (e.g., $(CH_3)_2COH^+$ reacting with N_2H_4). The reactants for experiment 7 (involving propanal and plotted in Figure 5a) lie approximately 18 kJ mol^{-1} above TSB. This is sufficient energy to traverse TSB to form hydrazonium and hydrazonium formation is observed experimentally. Reactants for experiment 8 (involving acetone and plotted in Figure 5b) lie approximatly 27 kJ mol^{-1} below TSB. These reactants do not have sufficient energy to traverse TSB, and no hydrazonium formation is observed.

TSA, which involves C−N bond formation, lies only slightly below the entrance channel. Although TSB governs hydrazone formation, TSA will determine whether structures such as II or those like III are representative of ions formed during thermal energy experiments. Experiment 10 indicates that the adduct ions undergo nucleophilic attack by N_2D_4. This result suggests that the adduct ions are represented by a structure such as II rather than III. This further suggests that TSA presents a kinetic barrier to reaction.[34] Starting from the higher energy reactants $CH_3CH_2CHOH^+/N_2H_4$ and $(CH_3)_2COH^+/N_2H_4$, TSA is more easily traversed.

b. Processes Involving Excess N_2H_4. Hydrazone forming reactions, such as experiments 3 and 5 where $N_2H_5^+$(CH_3CH_2-CHO) and N_2H_4 or $N_2H_5^+$(N_2H_4) and CH_3CH_2CHO are the

(32) Meot-ner (Mautner), M. In *Gas-Phase Ion Chemistry*; Bowers, M., Ed.; Academic Press: New York, 1979.

(33) Steinfeld, J. I.; Francisco, J. S.; Hase, W. L. *Chemical Kinetics and Dynamics*, 2nd ed.; Prentice Hall: Upper Saddle River, NJ, 1999.

(34) Olmstead, W. N.; Brauman, J. I. *J. Am. Chem. Soc.* **1977**, *99*, 4219−4228.

(35) Spanel, P.; Ji, Y.; Smith, D. *Int. J. Mass Spectrom. Ion Processes* **1997**, *165/166*, 25−37.

(36) Lide, D. R., Ed. *CRC Handbook of Chemistry and Physics*, 82nd ed.; CRC Press: Boca Raton, 2001.
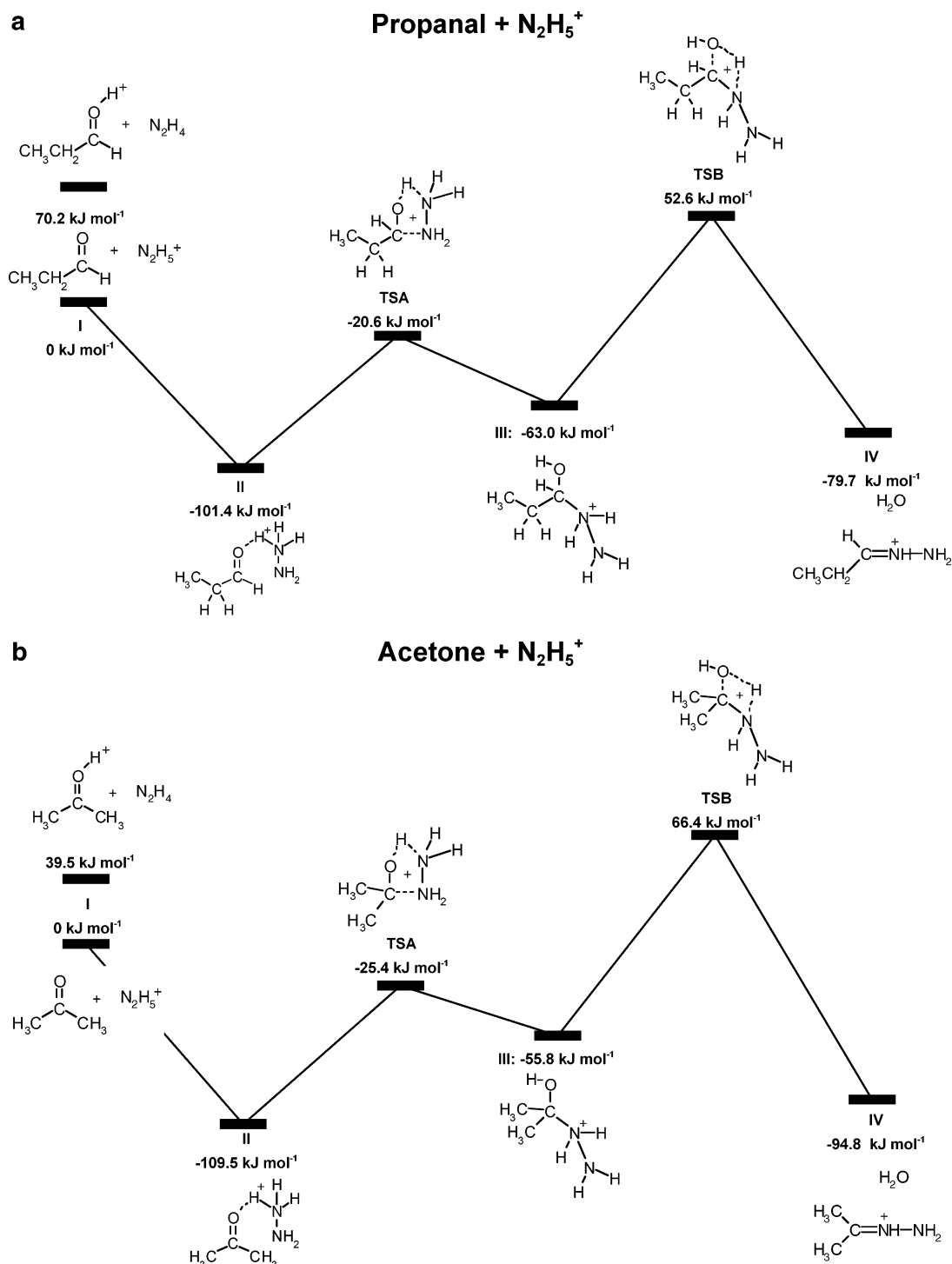
Figure 5. (a) Potential energy diagram for the reaction between propanal and $N_2H_5^+$ in the gas-phase described by Scheme 4. Also see Schemes 3 and 4 for simple chemical structures for these species. Labels including the letters "TS" indicate a transition state. (b) Potential energy diagram for the reaction between acetone and $N_2H_5^+$ in the gas-phase. Also see Schemes 3 and 4 for simple chemical structures for these species. Labels including the letters "TS" indicate a transition state.

reactive pairs, incorporate an extra molecule of N_2H_4 as compared to reaction between $N_2H_5^+$ and a carbonyl. Until new calculations are produced to treat this system directly, analogies to Figures 5a and 5b must aid in explaining the influence of this third molecule on hydrazone formation. By inclusion of the third molecule of N_2H_4 (or N_2D_4 for experiment 10), both the kinetic barrier to C−N bond formation, TSA, and the energetic barrier to proton transfer and loss of water, TSB, must be traversed more easily. For the bimolecular reaction between

$N_2H_5^+$ and a carbonyl, the nucleophilic nitrogen atom of structure II is somewhat constrained in its attack on the carbonyl carbon, being tethered at its opposite end through a proton to the carbonyl oxygen. A free molecule of N_2H_4, in the case of reaction between $N_2H_5^+(CH_3CH_2CHO)$ and N_2H_4, is more likely to succeed at nucleophilic attack and C−N bond formation since either of the N atom lone pairs can act as a nucleophile with less steric contraint. When $N_2H_5^+(N_2H_4)$ and CH_3CH_2CHO are the reactants, the N_2H_4 of the proton bound dimer is similarly

Scheme 6. Possible Concerted or Stepwise Paths toward Proton Transfer and Loss of Water in Propanal/N₂H₅⁺/N₂H₄ System^a
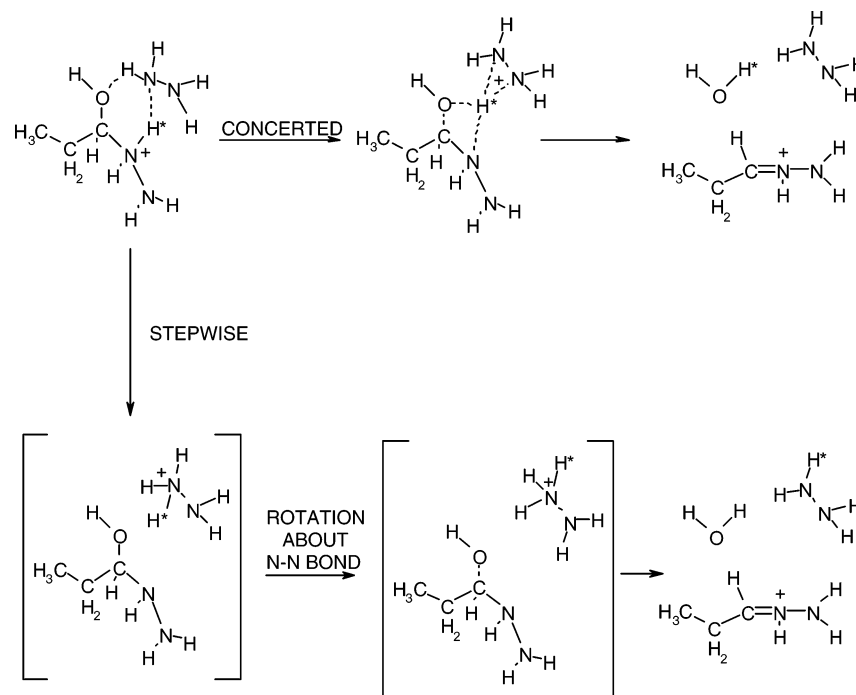

^{a} Stepwise path results in ambiguous position of H* atom in final products.

freed for nucleophilic attack. The presence of N_2H_4 therefore aids in reducing the barrier height via a new transition state (e.g., TSC, Scheme 3) and results in production of species III clustered to N_2H_4. For the acetone intermediate, the additional alkyl substituent on the carbonyl carbon may adversely affect nucleophilic attack by N_2H_4 due to steric hindrance and/or through inductive electron donation. These effects may contribute to the greater propensity toward hydrazonium formation of propanal compared to acetone that is observed experimentally.

In reactions between $N_2H_5^+(CH_3CH_2CHO)$ and N_2H_4 or $N_2H_5^+(N_2H_4)$ and CH_3CH_2CHO, the reactants will have available the ion–neutral association energy to assist in proton transfer leading to hydrazone formation. Such proton transfer may be a concerted process where the N_2H_4 moiety simply guides a proton in its migration to the carbonyl oxygen. It may also be a stepwise process where proton transfer to N_2H_4 occurs within a long-lived complex, followed by transfer of a proton to the carbonyl oxygen. For the latter process, rotation about the N–N bond in the $N_2H_5^+$ species may occur, followed by delivery of any one of three protons to the carbonyl oxygen. Both possibilities are pictured in Scheme 6. Further work is needed to ascertain which of these processes is more likely.

c. Hydrazone-Forming Reactions. Scheme 7 summarizes the processes resulting in hydrazone formation in this and prior studies. Pathways with solid arrows show hydrazone formation from a chemically or translationally activated complex involving only one N_2H_4. Pathways with dashed arrows show the process of hydrazone formation at thermal energies in the presence of a second N_2H_4. The combination of solid and dashed arrow paths indicates active processes for translational activation in the presence of excess N_2H_4.

Following collision of reactants A, carbonylH⁺ and N_2H_4, a chemically activated complex C is formed. The structure of this complex may vary depending on molecular orientation and energy during collision. Various paths toward product formation

Scheme 7. Routes to Hydrazone Formation at Thermal Energy (in the presence of N₂H₄), Following Translational Activation and Following Chemical Activation^a
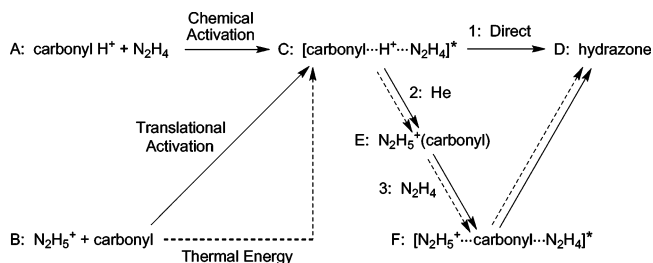
^{a} Competing paths not resulting in hydrazone formation are not shown.

will be available. The most favorable process is separation into $N_2H_5^+$ and a carbonyl (reactants B) as observed from experiment 7, Figure 4. Hydrazone formation is a minor process that occurs when a nucleophilic nitrogen lone pair comes in close proximity to the carbonyl carbon. Since no $N_2H_5^+$(carbonyl) clusters are observed, there is no significant collisional relaxation of the activated complex from this reactant pair.

Beginning with reactants B, $N_2H_5^+$ and a carbonyl in the presence of a drift field, a highly activated complex C may form. This energetic complex can react as described above although its excess internal energy is derived from translational activation rather than chemical activation. Beginning with reactants B, $N_2H_5^+$ and a carbonyl at thermal energies, a collision complex C will be formed with lower energy than those formed by the chemically or translationally activated paths. This complex will have a longer lifetime and will also have fewer available channels for product formation, as indicated with dashed arrows. In this case, collisional stabilization competes effectively with back dissociation into reactants B, $N_2H_5^+$ and a carbonyl. Most of these adducts will have a structure like II in Figures 5a or 5b and will not traverse TSA to yield structure III. In the presence of excess N_2H_4, the thermalized adduct may

form a new collision complex F. We have postulated that collisions involving clusters such as $N_2H_5^+$(carbonyl) with N_2H_4 or $N_2H_5^+$(N_2H_4) with a carbonyl will have reduced barriers to hydrazone formation. In addition, the internal energy from the ion−neutral complexation will promote hydrazone formation. Collisional relaxation of complex F competes effectively with hydrazone formation and results in production of the trimer, $N_2H_5^+$(N_2H_4)(carbonyl), as can be seen in Figures 1c and 2b.

Conclusions

Experiments using the SIFT-CIMS instrument and theoretical calculations have aided in developing a mechanism of hydrazone formation from protonated gas-phase hydrazine and carbonyls. Experiments demonstrated the role of neutral hydrazine in attacking the carbonyl carbon as well as differences in reactivity between aldehydes and ketones. Calculations reveal that the transition state involving nucleophilic attack and C−N bond formation presents a kinetic barrier to hydrazone formation in the reaction between $N_2H_5^+$ and a carbonyl. A second transition state, involving proton transfer and loss of water, also presents an energetic barrier to reaction and is key to hydrazone formation. The reaction between the $N_2H_5^+$(aldehyde) complex and a second N_2H_4 follows a different path with lower barriers. N_2H_4 also participates in proton-transfer and water loss via either a concerted or stepwise mechanism within an energetic ion/molecule reaction complex. The greater propensity of propanal toward hydrazone formation than acetone may be related to either of these transition states and likely involves both steric and inductive electron donation effects.

For higher carbonyls, the rate coefficient for adduct formation, which should be followed by hydrazone formation, is comparable in magnitude to that of proton transfer reactions. These proton transfer reactions occur at collisional rates and have been used to detect trace species in the pptv concentration range. Adduct formation rate coefficients will approach their collisional values as pressure is increased. The process of hydrazone formation is likely rate limiting and will determine the rate with which hydrazones are produced at thermal energies although even this process is rapid. Hydrazone formation rates and yields may increase under drift-field conditions. Future experiments may include calculation of the $N_2H_5^+$(carbonyl)(N_2H_4) system as well as an experimental investigation of the reactions between $N_2H_5^+$ and a carbonyl in the presence of a drift field but in the absence of excess N_2H_4. Further measurement of the reaction rate coefficient for hydrazone formation from reaction between $N_2H_5^+$(carbonyl) adducts and N_2H_4, without interference from $N_2H_5^+$, would also be valuable. It is hoped that these results will aid in future exploration of the energetics and kinetics of hydrazone formation in the gas phase under drift conditions and for a variety of species. These results should also encourage the use of $N_2H_5^+$ as a CIMS reagent for selective, on-line monitoring of trace carbonyls in a variety of settings and instruments.

Supporting Information Available: Discussion of the observed production and loss of NH_3^+ and NH_4^+; experimentally derived and calculated proton affinities of carbonyl compounds, ammonia, and hydrazine; anticipated switching reactions of clusters involving hydrazine, water, and carbonyls; z-matrices, energies, energy diagrams, and structures for each species investigated computationally. This material is available free of charge via the Internet at http://pubs.acs.org.

JA0350886